THE ASTROPHYSICAL JOURNAL, 559:L123–L126, 2001 October 1

KECK MEASUREMENT OF THE XTE J2123−058 RADIAL VELOCITY CURVE

JOHN A. TOMSICK,[1] WILLIAM A. HEINDL,[1] DEEPTO CHAKRABARTY,[2] JULES P. HALPERN,[3] AND PHILIP KAARET[4]

Received 2001 June 26; accepted 2001 August 13; published 2001 September 6

ABSTRACT

We measured the radial velocity curve of the companion of the neutron star X-ray transient XTE J2123−058. Its semiamplitude (K_2) of 298.5 ± 6.9 km s^{-1} is the highest value that has been measured for any neutron star low-mass X-ray binary. The high value for K_2 is, in part, due to the high binary inclination of the system but may also indicate a high neutron star mass. The mass function (f_2) of $0.684 \pm 0.047\ M_\odot$, along with our constraints on the companion's spectral type (K5 V–K9 V) and previous constraints on the inclination, gives a likely range of neutron star masses from 1.2 to 1.8 $M_\odot$. We also derive a source distance of 8.5 ± 2.5 kpc, indicating that XTE J2123−058 is unusually far, 5.0 ± 1.5 kpc, from the Galactic plane. Our measurement of the systemic radial velocity is −94.5 ± 5.5 km s^{-1}, which is significantly different from what would be observed if this object corotated with the disk of the Galaxy.

Subject headings: accretion, accretion disks — stars: individual (XTE J2123−058) — stars: neutron — X-rays: general — X-rays: stars

1. INTRODUCTION

The X-ray transient XTE J2123−058 is a neutron star low-mass X-ray binary (LMXB) that was discovered in 1998 (Levine, Swank, & Smith 1998). We optically identified the transient (Tomsick et al. 1998a) and determined the ~6 hr binary orbital period (Tomsick et al. 1998b). Type I X-ray bursts indicate that the system contains a neutron star, and the relatively short orbital period indicates that the companion is a late-type star on or close to the main sequence. A pair of high-frequency quasi-periodic oscillations was detected, which may indicate a rapidly rotating neutron star (Homan et al. 1999; Tomsick et al. 1999). XTE J2123−058 distinguishes itself from other LMXBs by having high Galactic latitude ($b = -36°$) and also a high binary inclination ($i \sim 73°$; Zurita et al. 2000). Both of these properties are advantageous for determining the mass of the neutron star from optical observations in quiescence, which is the primary goal of this work.

Such mass measurements are important for constraining neutron star equations of state and for understanding the evolution of neutron star systems. Precise mass measurements have been made for millisecond radio pulsars (MSPs; Thorsett & Chakrabarty 1999), but these measurements are lacking for LMXBs. Since it is theoretically possible to spin up neutron stars in LMXBs to millisecond periods via accretion, a link between LMXBs and MSPs has long been suspected (Alpar et al. 1982). Although there is substantial evidence to support this picture, the prediction that rapidly rotating neutron stars in LMXBs should be more massive by 0.1–0.5 $M_\odot$ (Bhattacharya 1995) than those that have not been spun up has not been tested.

2. OBSERVATIONS AND DATA REDUCTION

In 2000 August, we performed spectroscopy of XTE J2123−058 with the Echelle Spectrograph and Imager (ESI; Sheinis et al. 2000) at the Keck Observatory. As shown in Table 1, we took eight exposures over two nights covering the 6 hr binary orbit. The cross-dispersed spectra were taken in echelle mode with 10 spectral orders falling on a 2048 × 4096 pixel CCD. We performed on-chip rebinning to 2048 × 2048 pixels to decrease read noise. Although this instrument is sensitive from 3900 to 11000 Å, we only used the data in the 4700–6820 Å band where the dispersion varies from 0.36 to 0.52 Å per rebinned pixel. This is sufficient to oversample the resolution of the spectrograph since we used a 1″ slit, providing a spectral resolution of 1.0–1.5 Å FWHM.

We obtained *R*- and *V*-band photometry of XTE J2123−058 at the MDM Observatory 10 days before the Keck observations and found values for *R* and *V* consistent with the quiescent magnitudes reported in Tomsick et al. (1999). We measured $V = 22.68 \pm 0.11$ (corrected for atmospheric extinction but not reddening), and we use this value below to determine the source distance. Due to the faintness of the source, relatively long exposure times between 2340 and 2700 s were necessary for our spectroscopic observations. Even these exposures are a relatively small fraction of the orbital period. We obtained M, K, and G dwarf comparison star spectra for the cross-correlations described below.

We extracted the spectra using the software package "MAKEE" that was originally developed for the HIRES instrument at Keck but has been adapted to extract ESI spectra. Using MAKEE, we produced optimally extracted spectra for each of the 10 spectral orders. We obtained CuAr line lamp exposures to determine the wavelength solution, and we checked this solution for each exposure using O I and Na I night-sky lines. Averaging over all exposures and night-sky lines, the difference between measured and actual wavelengths is 0.018 Å. The calibration is also stable from exposure to exposure with a standard deviation of 0.027 Å or less for all night-sky lines, corresponding to a radial velocity measurement error of less than 1.5 km s^{-1}. The data reduction procedure includes heliocentric velocity and atmospheric extinction corrections. We used IRAF routines to flux-calibrate the spectra and obtained exposures of the spectrophotometric standard

---

[1] Center for Astrophysics and Space Sciences, Code 0424, 9500 Gilman Drive, University of California at San Diego, La Jolla, CA 92093-0424; jtomsick@ucsd.edu.

[2] Department of Physics, 77 Massachusetts Avenue, and Center for Space Research, 70 Vassar Street, Building 37, Massachusetts Institute of Technology, Cambridge, MA 02139.

[3] Columbia Astrophysics Laboratory, Columbia University, 550 West 120th Street, New York, NY 10027.

[4] Harvard-Smithsonian Center for Astrophysics, 60 Garden Street, Cambridge, MA 02138.

TABLE 1

XTE J2123−058 Keck Observations

Exposure	MJD[a] (days)	Exposure Time (s)	FWHM Seeing (arcsec)
1	51759.39442	2700	0.87
2	51759.42822	2510	0.91
3	51759.45771	2510	1.23
4	51759.48768	2510	0.79
5	51759.51748	2400	0.85
6	51759.54536	2340	0.98
7	51759.57288	2340	0.86
8	51760.35770	2400	0.67

[a] Modified Julian Date (JD−2,400,000.5) at the midpoint of the exposure.

TABLE 2

Fluxes, S/Ns, and Cross-Correlation Results

Exposure	Flux[a]	S/N[b]	R[c]	Measured RV[d]	Fitted RV[e]
1	1.24	1.66	3.26	55.3 ± 17.6	63.2
2	1.72	2.66	4.29	−191.0 ± 22.7	−182.4
3	1.53	2.15	4.54	−298.1 ± 24.6	−352.8
4	2.90	4.40	8.88	−390.1 ± 12.2	−385.0
5	3.06	4.18	8.82	−265.2 ± 12.5	−259.0
6	2.48	2.87	5.14	−69.6 ± 17.3	−58.1
7	2.32	2.41	3.35	192.2 ± 25.0	123.6
8	5.53	6.63	16.32	191.0 ± 7.4	193.5

[a] Mean flux in the 5650–5850 Å band in units of 10^{-18} ergs cm^{-2} s^{-1} Å^{-1}.

[b] Mean S/N per pixel in the 5650–5850 Å band.

[c] Tonry & Davis 1979 R-value.

[d] Measured heliocentric radial velocity in kilometers per second with Tonry & Davis 1979 errors.

[e] Heliocentric radial velocity in kilometers per second based on a sinusoidal fit to the data.

Hiltner 102 (Stone 1977) on both nights for this purpose. We combined the spectral orders after flux calibration and rebinned the spectra to a logarithmic wavelength scale with 22.8 km s^{-1} pixels. Finally, we dereddened the XTE J2123−058 spectra using $A_V = 0.37$ mag (Hynes et al. 2001).

The quality of the XTE J2123−058 spectra varies significantly between exposures, as indicated by the signal-to-noise ratios (S/Ns) given in Table 2. The mean S/N per pixel in the 5650–5850 Å band is 1.66 in the worst case and 6.63 in the best case. One reason for this is that the source shows large orbital flux variations, as can be seen from the fluxes given in Table 2. The flux variations show two peaks per orbit (exposures 5 and 8), which is expected if the variability is due to ellipsoidal modulations. XTE J2123−058 light curves from optical photometry show that ellipsoidal modulations are indeed present (Zurita et al. 2000). The S/N variations are also caused by variable seeing, as shown in Table 1. The FWHM seeing for the exposure taken on the second night is 0″.67 compared with an average of 0″.93 for the exposures on the first night. It should be noted that the Table 2 fluxes are not corrected for seeing.

3. RESULTS

3.1. *Cross-Correlations*

Our analysis of the spectra focuses on the region from 4700 to 6820 Å since the S/N becomes very poor below 4700 Å and since night-sky lines dominate the spectrum above 6820 Å. In this band, the spectra show features from the accretion disk (Hα and Hβ emission lines) and from the companion star. An examination of the spectra clearly shows the presence of a wide depression centered between 5100 and 5200 Å. This is the signature of a K-type star and is due to the MgH feature at 5180 Å, the TiO band at 4954–5200 Å, and a continuum discontinuity associated with the Mg I triplet at 5168–5185 Å (McClintock & Remillard 1990 and references therein). An absorption feature is seen near 5900 Å that is due to the Na I doublet at 5891–5898 Å. The strength of this feature indicates a late-K spectral type for the companion.

We used the IRAF routine "FXCOR" (Tonry & Davis 1979; Filippenko, Matheson, & Ho 1995) to cross-correlate the XTE J2123−058 spectra with the comparison stars. After masking night-sky lines at 5205, 5579, 5891, 5898, and 6302 Å and the Hα and Hβ emission lines from the source, we used the wavelength bands 4890–5190, 5210–5560, 5630–5860, 5985–6135, and 6640–6820 Å for the cross-correlations. We also applied a bandpass filter from 30 to 800 cycles per spectrum in order to remove contributions due to spurious variations in the continuum and high-frequency noise. We calculated cross-correlations for G0 V, G5 V, G9 V, K0 V, K2 V, K4 V, K7 V, M0 V, and M1 V with the exposure 8 spectrum. Highly significant peaks with Tonry & Davis (1979) R-values between 8.9 and 16.3 at roughly the same velocity occur, with the M-type and G0 V stars giving the weakest correlations and the K7 V star (HD 88230) giving the strongest correlation. For this reason and because of the

TABLE 3

Spectroscopic Parameters

Parameter	Result[a]
Epoch[b]	T_0 = HJD 2,451,760.0462 ± 0.0013 days
Systemic velocity	$\gamma = -94.5 \pm 5.5$ km s^{-1}
Velocity semiamplitude	$K_2 = 298.5 \pm 6.9$ km s^{-1}
Orbital period[c]	$P_{\rm orb} = 21445.5$ s

[a] 68% confidence errors are given.

[b] Heliocentric Julian Date of the epoch of inferior conjunction.

[c] Orbital period determined from photometry (Tomsick et al. 1999; Ilovaisky & Chevalier 1998; Zurita et al. 2000).

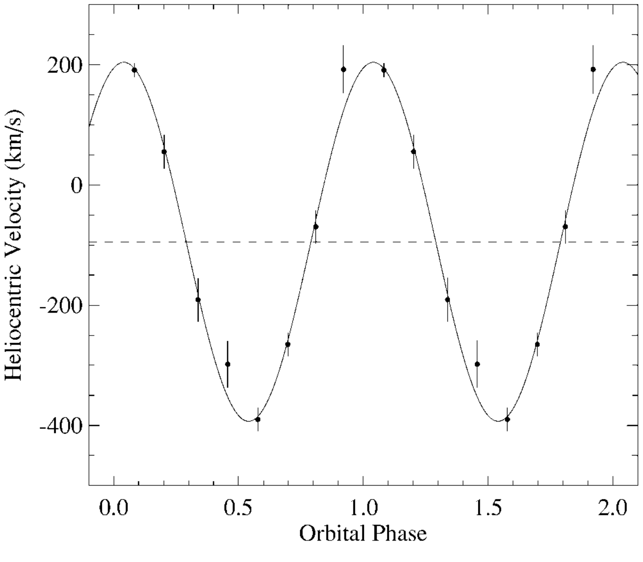

Fig. 1.—Radial velocity curve fitted using a sinusoid with the parameters given in Table 3 and folded on the orbital period. Heliocentric velocities are shown (with errors increased by 60% over the values given in Table 2), and the dashed line marks the systemic velocity. The data are plotted twice for clarity.

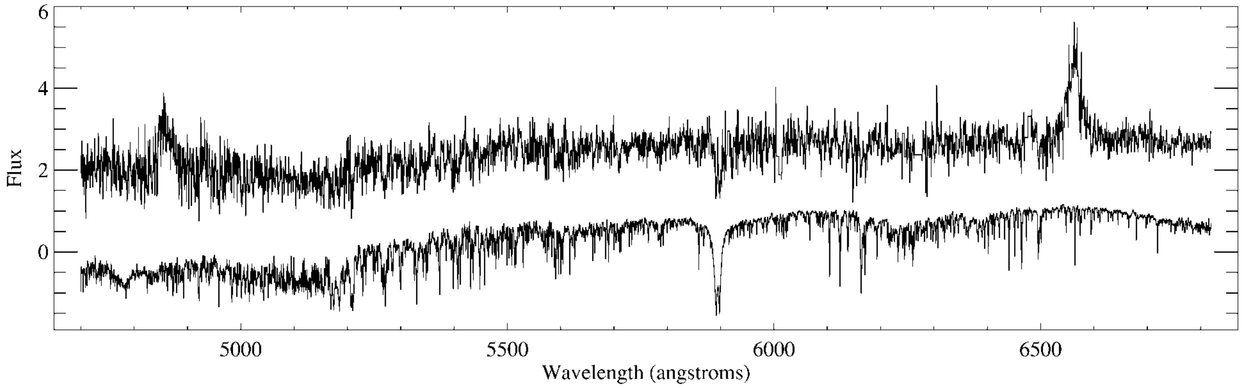

FIG. 2.—The top spectrum shows the average, Doppler-corrected spectrum for XTE J2123−058 in units of 10^{-18} ergs cm^{-2} s^{-1} Å^{-1}. Hα and Hβ emission lines are present at 6564 and 4863 Å. The spectrum for the K7 V comparison star (HD 88230) is shown below, and the units are arbitrary. Several matching features between XTE J2123−058 and HD 88230 are present, including the continuum break near 5200 Å and the Na I doublet at 5891–5898 Å.

strong Na I line, we used the K7 V star for the radial velocity study.

We obtained unique and significant cross-correlation peaks at reasonable velocities (−1000 to 1000 km s^{-1}) for all eight exposures. The measured heliocentric velocities range from −390 to 192 km s^{-1} and are given in Table 2. The R-values vary significantly from 3.3 to 16.3 because of S/N differences. Figure 1 shows the radial velocity curve. First, we performed a least-squares fit to the data with a function consisting of a constant plus a sinusoid with four free parameters: the systemic velocity (γ), the epoch of inferior conjunction (T_0), the radial velocity semiamplitude (K_2), and the orbital period ($P_{\rm orb}$). This does not provide a formally acceptable fit ($\chi^2/\nu = 12/4$), so we increased the errors on the individual velocity measurements by 60% to give a reduced χ^2 of 1.0. The fit gives a large range of possible values for $P_{\rm orb}$ with a 90% confidence error region from 21125 to 22575 s. This range contains the photometric orbital period of 21445.5 ± 2.3 s measured previously (Tomsick et al. 1999; Ilovaisky & Chevalier 1998; Zurita et al. 2000), and we refitted the radial velocity curve after fixing $P_{\rm orb}$ to this value. We expect that the photometric and spectroscopic orbital periods are the same since the photometric value is based on partial eclipses seen in the optical light curve during outburst (Tomsick et al. 1999; Zurita et al. 2000).

Table 3 shows the fit parameters with $P_{\rm orb}$ fixed, and this fit is shown in Figure 1. Its semiamplitude (K_2) of 298.5 ± 6.9 km s^{-1} is the highest value that has been measured for any neutron star LMXB. The value of −94.5 ± 5.5 km s^{-1} for γ is consistent with the tentative value of −90 km s^{-1} derived from emission lines (Hynes et al. 2001). We note that previous measurements of the photometric epoch are too uncertain to make a meaningful comparison with our spectroscopic epoch.

3.2. *Average Spectrum and Source Distance*

We produced an average, Doppler-corrected spectrum using the eight XTE J2123−058 exposures. We first removed pixels contaminated by night-sky lines. Next, we multiplied each spectrum by a constant based on the fluxes given in Table 2 to establish a common normalization. This is important because the wavelength bins near night-sky lines do not have contributions from all eight exposures. We then Doppler-corrected the spectra using the fitted radial velocity values given in Table 2. Finally, we interpolated the spectra to a common set of wavelength bins and calculated the weighted average for each wavelength bin.

The average spectrum is shown in Figure 2 along with the spectrum of HD 88230. Gaussian fits to the XTE J2123−058 emission lines give equivalent widths (EWs) of 15.8 and 17.6 Å and FWHMs of 1443 ± 64 and 1729 ± 133 km s^{-1} for Hα and Hβ, respectively. The FWHMs are significantly less for the individual exposures. The continuum features near 5000–5300 Å are similar to HD 88230, and narrow Mg I absorption lines are seen in both spectra near the break in the continuum. Matching absorption lines are also present in several other parts of the spectrum, including the Na I doublet at 5891–5898 Å.

We fitted the region of the spectrum near the Na I doublet with a constant plus two inverted Gaussians for the XTE J2123−058 average spectrum and also for the comparison stars in order to determine the total EW of the Na I doublet. For XTE J2123−058, we measure an EW of 3.1 ± 0.6 Å (after correcting for interstellar absorption using results from Hynes et al. 2001). For the K0 V, K2 V, K4 V, K7 V, and M1 V comparison stars, we measure EWs of 1.1, 2.5, 3.6, 6.9, and 7.2 Å, respectively. Since the Hα and Hβ emission lines indicate a significant disk contribution, these EW values indicate that the spectral type of the companion is later than K4 V. However, based on the strengths of the cross-correlation peaks described above, the companion is a K- rather than an M-type star. The range of possible spectral types is K5 V–K9 V.

We determined the source distance using the method described by McClintock et al. (2001). We assume a spectral type of K7 V in the calculation and discuss possible associated uncertainties below. The strength of the Na I doublet indicates that the fraction of the light coming from the companion at 5900 Å is 45% ± 8%. This, along with the MDM measurement ($V = 22.68$), gives an effective V magnitude for the companion of 23.56. We calculated the absolute V magnitude (M_V) of the companion using the expression given in Popper (1980), which depends on the spectral type and the radius of the companion. Since the companion fills its Roche lobe, its average density depends only on the orbital period (Faulkner, Flannery, & Warner 1972). From the density and assuming that the companion mass is 0.4 $M_\odot$, which is likely correct to within a factor of 2 (Barret, McClintock, & Grindlay 1996), we estimate a radius of 0.56 $R_\odot$ for the companion. This radius and the K7 V spectral type give $M_V = 8.42$. After accounting for extinction, we obtained a source distance of 9.0 kpc. Recalculating with different spectral types indicates that the error associated with the

K5 V–K9 V range is ±1 kpc. Also, the factor of 2 uncertainty in the companion's mass translates to a 25% uncertainty in the distance (McClintock et al. 2001). Finally, there is a systematic error due to orbital variations in the *V* magnitude. The MDM observations were made close to photometric minimum, so that the average *V* magnitude is somewhat less than 22.68. Based on the quiescent light curve shown in Zurita et al. (2000), we estimate that the average *V* magnitude is close to 22.55, which decreases the distance by 0.5 kpc. We conclude that the distance is 8.5 ± 2.5 kpc, indicating that XTE J2123−058 is 5.0 ± 1.5 kpc from the Galactic plane.

4. DISCUSSION AND CONCLUSIONS

From K_2 and $P_{\rm orb}$, we derive a mass function of $f_2 = 0.684 \pm 0.047\ M_\odot$, representing a lower limit on the neutron star mass (M_1). The binary inclination (i) and the mass ratio ($q = M_1/M_2$) are also necessary to obtain a precise measurement of M_1. For XTE J2123−058, $i = 73° \pm 4°$ was determined via modeling of the outburst optical light curves (Zurita et al. 2000). Figure 3 shows M_1 versus M_2 using the measured values of f_2 and i. From our constraint on the spectral type of the companion (K5 V–K9 V), it is very likely that M_2 lies between 0.4 and 0.7 $M_\odot$. For this range of companion masses, the range of neutron star masses is 1.2–1.8 $M_\odot$. An accurate determination of q, which may be possible via measurements of the rotational broadening of the secondary or light-curve modeling, is critical to improve the mass constraint. Finding that the neutron star mass is near the upper end of the 1.2–1.8 $M_\odot$ mass range would have important implications for neutron star equations of state, and, in general, determining the mass has important implications for the evolution of neutron star systems.

The source distance we obtain is consistent with previous estimates (Homan et al. 1999; Tomsick et al. 1999), confirming that XTE J2123−058 is unusually far from the Galactic plane and implying a bolometric luminosity between 3×10^{37} and 10^{38} ergs s^{-1} for the brightest X-ray bursts detected during the 1998 outburst (Tomsick et al. 1999). Given the distance and longitude ($l = 46.5°$) of XTE J2123−058, the systemic radial velocity of −94.5 km s^{-1} is significantly different from what would be observed for an object corotating with the disk of the Galaxy. This fact alone does not allow us to distinguish between a scenario in which the source was ejected from the Galactic plane and the possibility that XTE J2123−058 has a halo origin.

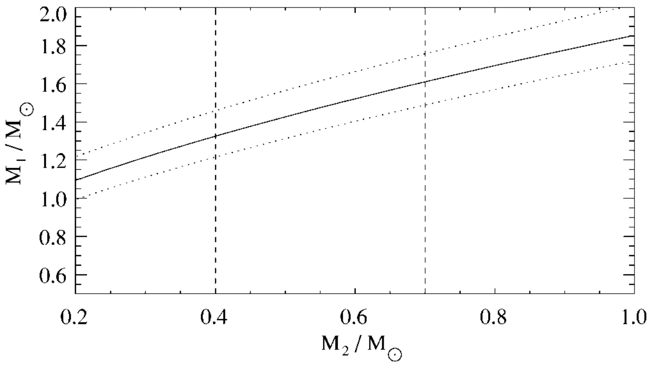

FIG. 3.—Neutron star mass (M_1) vs. the companion mass (M_2). The solid line comes from the values of f_2 and i given in the text, and the dotted lines are based on the extremes of the error regions for these parameters. The vertical dashed lines mark the likely range for M_2.

We wish to thank John O'Meara for his help with observations and data reduction. We thank Tom Barlow for assistance with his MAKEE software. We acknowledge Judith Cohen for obtaining a standard star exposure for us and Bob Goodrich for his help with ESI. We thank Gary Puniwai and Charles Sorenson for assistance. Data for this work were obtained at the W. M. Keck Observatory, which is operated as a scientific partnership among the University of California, Caltech, and NASA.

REFERENCES

Alpar, M. A., Cheng, A. F., Ruderman, M. A., & Shaham, J. 1982, Nature, 300, 728
Barret, D., McClintock, J. E., & Grindlay, J. E. 1996, ApJ, 473, 963
Bhattacharya, D. 1995, X-Ray Binaries (Cambridge: Cambridge Univ. Press)
Faulkner, J., Flannery, B. P., & Warner, B. 1972, ApJ, 175, L79
Filippenko, A. V., Matheson, T., & Ho, L. C. 1995, ApJ, 455, 614
Homan, J., Méndez, M., Wijnands, R., van der Klis, M., & van Paradijs, J. 1999, ApJ, 513, L119
Hynes, R. I., Charles, P. A., Haswell, C. A., Casares, J., Zurita, C., & Serra-Ricart, M. 2001, MNRAS, 324, 180
Ilovaisky, S. A., & Chevalier, C. 1998, IAU Circ. 6975
Levine, A., Swank, J., & Smith, E. 1998, IAU Circ. 6955
McClintock, J. E., Garcia, M. R., Caldwell, N., Falco, E. E., Garnavich, P. M., & Zhao, P. 2001, ApJ, 551, L147
McClintock, J. E., & Remillard, R. A. 1990, ApJ, 350, 386
Popper, D. M. 1980, ARA&A, 18, 115
Sheinis, A. I., Miller, J. S., Bolte, M., & Sutin, B. M. 2000, Proc. SPIE, 4008, 522
Stone, R. P. S. 1977, ApJ, 218, 767
Thorsett, S. E., & Chakrabarty, D. 1999, ApJ, 512, 288
Tomsick, J. A., Halpern, J. P., Kemp, J., & Kaaret, P. 1999, ApJ, 521, 341
Tomsick, J. A., Halpern, J. P., Leighly, K. M., & Perlman, E. 1998a, IAU Circ. 6957
Tomsick, J. A., Kemp, J., Halpern, J. P., & Hurley-Keller, D. 1998b, IAU Circ. 6972
Tonry, J., & Davis, M. 1979, AJ, 84, 1511
Zurita, C., et al. 2000, MNRAS, 316, 137